Biogeosciences
Open Access
Discussions

CO$_2$ uptake of a mature *Acacia mangium* plantation estimated from sap flow measurements and stable carbon isotope discrimination

H. Wang[1], P. Zhao[2], L. L. Zou[2], H. R. McCarthy[3], X. P. Zeng[2], G. Y. Ni[2], and X. Q. Rao[2]

[1]Institute of Forestry and Pomology, Beijing Academy of Agriculture and Forestry Sciences, Beijing 100093, China
[2]Key laboratory of Vegetation Restoration and Management of Degraded Ecosystems, South China Botanical Garden, Chinese Academy of Sciences, Guangzhou 510650, China
[3]Department of Botany and Microbiology, University of Oklahoma, Norman, OK 73019, USA

Discussion Paper | Discussion Paper | Discussion Paper | Discussion Paper

BGD
10, 11583–11625, 2013

CO$_2$ uptake of a mature *Acacia mangium* plantation

H. Wang et al.

Title Page
Abstract | Introduction
Conclusions | References
Tables | Figures
◄ | ►
◄ | ►
Back | Close
Full Screen / Esc
Printer-friendly Version
Interactive Discussion

Full Screen / Esc

Printer-friendly Version

Interactive Discussion

Abstract

Canopy CO$_2$ uptake (F_{CO_2}) of a subtropical mature *A. mangium* plantation was estimated by combining sap flow measurements and stable carbon isotope discrimination (Δ) in Southern China from 2004 to 2007. The mechanistic relationship linking F_{CO_2},

5 Δ in leaf sap, and sap flow based canopy stomatal conductance (G_s) was applied in our study. No significant seasonal variations were observed in Δ or in the ratio of the intercellular and ambient CO$_2$ concentrations (C_i/C_a), although diurnal C_i/C_a varied between sunlit and shaded leaves. A sensitivity analysis showed that estimates of F_{CO_2} were more sensitive to dynamics in G_s than in C_a and Δ. By using seasonally and

10 canopy averaged C_i/C_a values, an acceptable estimate of F_{CO_2} was obtained. F_{CO_2} exhibited similar diurnal variation to that of G_s. Large seasonal variation in F_{CO_2} was attributed to the responsiveness of G_s to vapour pressure deficit, photosynthetically active radiation, and soil moisture deficit. Our estimate of F_{CO_2} for a mature *A. mangium* plantation (2.13±0.40 g C m^{-2} day^{-1}) approached the lower range of values for subtrop-

15 ical mixed forest, probably due to lower mean canopy stomatal conductance, higher C_i/C_a, and greater tree height than other measured forests. Our estimate was also lower than values determined by satellite-based modeling or component carbon analysis, suggesting the necessity of stand level flux data for verification. Qualitatively, the sap flux/stable isotope results compared well with gas exchange results. Differences in

20 results between the two approaches reflected variability due to leaf position and age, which could be reduced for sap flux/stable isotope, which uses canopy average values of G_s and C_i/C_a.

1 Introduction

The continued increase in atmospheric carbon dioxide levels due to anthropogenic

25 emissions has led to significant climate changes (Schneider, 1989). Rising atmospheric CO$_2$ is due to the imbalance between the rates that sources emit CO$_2$ into

the atmosphere and the rates that sinks remove CO$_2$ from the atmosphere (Baldocchi et al., 1996). In this context, forests act as vital CO$_2$ sinks by storing carbon in woody biomass (Nowak et al., 2002). It has been reported that forests at northern mid-latitude sites are large CO$_2$ sinks (Ciais et al., 1995). However, biomass increments are highly

5   variable with stand age, and many other factors, primarily resource availability (Oren et al., 2001; Peng, 2003). Additionally, studies have frequently shown that primary or mature forests reach a balance between C uptake and release, after which their further contribution to carbon fixation are no longer significant (Fang and Chen, 2001; Oren et al., 2001). However, estimation of canopy scale photosynthesis has been rel-

10 atively rare. Such uncertainties hinder our ability to estimate forest CO$_2$ sequestration for global carbon budgets, as well as to increase CO$_2$ sequestration through forest management.

   Canopy is an important intermediate scale between leaf and ecosystem. Although established photosynthesis monitoring techniques are available for both leaf and

15 ecosystem scale (Farquhar et al., 1980; Baldocchi et al., 1996), there is currently no commonly accepted estimation method for photosynthesis at the canopy scale. This limits our understanding of canopy photosynthesis compared with canopy water fluxes, which can be determined through sap flow techniques. A number of methods have been designed to address the dilemma, including (1) combining water use efficiency

20 obtained with branch bag techniques and whole-tree transpiration (Morén et al., 2001), (2) coupling between sap flow-based canopy stomatal conductance and photosynthesis (Catovsky et al., 2002), and (3) using a canopy conductance constrained carbon assimilation scheme, which couples actual or potential canopy conductance with vertical gradients of light distribution, leaf-level conductance, maximum Rubisco capacity

25 and maximum electron transport (Schäfer et al., 2003; Kim et al., 2008). However, application of these methods still requires extensive leaf gas exchange measurements, which are time-consuming and difficult, because access to tall canopies is required. Recently, a novel approach combining sap flow measurement and stable carbon isotope techniques was proposed to estimate forest CO$_2$ uptake (Zhao et al., 2005a).

By virtue of continuous measurements of sap flow, the instantaneous CO_2 uptake rate of a forest can be estimated based on the relationship between sap flow measurement-derived canopy stomatal conductance and ^{13}C discrimination. This new approach is unique in its continuity, representativeness, accuracy and ease of use: canopy stomatal conductance is derived from continuous measurement of sap flow (Zhao et al., 2005a); the relationship of net photosynthetic rate/canopy stomatal conductance (A_{net}/G_s) derived from stable carbon isotope discrimination (Δ) is very stable and representative on both temporal and spatial scales (Dawson et al., 2002); and sap flow measurement is non-destructiveness, easy, and low cost (Granier, 1987; Zhao et al., 2005b). Additionally, this sap flux/stable isotope combination is advantageous compared to approaches that rely on up-scaling of leaf-level measurements, or partitioning of eddy covariance fluxes. It could avoid the errors frequently associated with modeling of CO_2 fluxes, and facilitate continuous data streams which are particularly suitable for field measurement of forests in mountainous areas (Zhao et al., 2005a). Given these features, we hypothesize that with appropriate sampling the variability of the relationship of A_{net}/G_s on both temporal and spatial scales can be integrated to achieve a representative, instantaneous value of CO_2 uptake at the canopy scale. We also hypothesize that CO_2 uptake obtained from this novel approach is comparable to, and consistent with results from other methods. Hereby, the stem sap flux, carbon isotopic compositions of leaf sap, and environmental parameters in a subtropical *A. mangium* plantation in Southern China were measured from 2004 to 2007. It was intended: (1) to provide an alternative sap flow-based method for estimating instantaneous CO_2 uptake at the canopy scale and be verified by comparing with those obtained from other methods, which could be used to (2) investigate the diurnal, seasonal, annual and inter-annual changes of CO_2 uptake of the plantation and (3) examine how CO_2 uptake of the plantation is regulated by the stomata and environmental conditions. We expected that F_{CO_2} of a subtropical mature *A. mangium* plantation could be estimated by the sap flux/stable isotope combination. We also expected that F_{CO_2} would

be more sensitive to changes in G_s than in C_a and Δ. Finally, we expected that the F_{CO_2} would be highest in the mid-morning during summer months.

2 Materials and methods

2.1 Site description and environmental conditions

This study was conducted at the Heshan Hilly Land Interdisciplinary Experimental Station of the Chinese Academy of Sciences (112°54′ E, 22°41′ N) in Guangdong Province, China over the 2004–2007 period. The study site is dominated by a subtropical monsoonal climate with the wet season occurring from April to September and the dry season from October to March. Mean annual temperature is 21.7 °C and average precipitation is 1400 mm, of which 78 % occurs in the wet season.

The study stand is situated at 60–70 m altitude, on a 20° slope with a south-east aspect. The soil is an oxisol developed from sandstone with surface soil to a depth of 10 cm and subsoil for a further 50 cm (Ma et al., 2008a). *Acacia mangium* is a fast-growing legume species that has nitrogen fixing nodules on its shallow roots (Cole et al., 1996). It was introduced to China from Southeast Asia in the late 1970s and has been widely used for restoration of vegetation in tropical and subtropical China (Yang et al., 2009). *A. mangium* reach maturity after ∼ 20 yr of growth. *Acacia mangium* was the only overstory species planted at a spacing of 3 m × 4 m in 1984. The understory vegetation is very sparse and its contribution to stand CO_2 uptake was considered to be negligible for the purposes of this study. A study plot with an area of 640.5 m^2 (36.6 m × 17.5 m) was set up within the stand. The plot comprised 47 trees (734 trees per hectare) with a basal area of 26.6 m^{-2} ha^{-1}. Tree height ranged from 2.4 m to 22.8 m with an average of 15.7 m. Stem diameter at breast height (DBH) was between 3.8 cm and 37.5 cm with an average of 20.1 cm. The projected canopy area (A_c) was estimated to range from 0.8 m^2 to 53.0 m^2 with an average of 13.8 m^2. Fourteen trees, representative of the DBH distribution in the plot, were selected, for sap flow measurement, with tree

height ranging from 12 m to 22.8 m, DBH between 13.4 and 37.5 cm and A_c ranging from 4.6 m^2 to 47.7 m^2 (Table 1).

Air temperature (T_a, °C), air relative humidity (RH, %), and photosynthetically active radiation (PAR, µmol m^{-2} s^{-1}), were monitored in a weather station located 150 m away from the study site. T_a and RH were measured using a HMP35E sensor (HMP35E; Vaisala, Finland). PAR was measured with a LI-190SA quantum sensor (Li-Cor, Lincoln, US). Since the root system of *A. mangium* is mainly distributed in the upper 30 cm of the soil, volumetric soil water content (SWC, m^3 m^{-3}) was measured using three soil moisture probes (ML2x, Delta-T Device, UK) inserted into the upper soil (20–30 cm) amongst the selected trees. The environmental data were sampled and recorded as 10 min means by a data logger synchronized to the logger for sap flow measurements. Vapor pressure deficit (D) was calculated from T_a and RH as follows:

$$D = a \times \exp\left[\frac{bT_a}{(T_a + c)}\right] \times (1 - \text{RH}) \tag{1}$$

where a, b, and c are fixed parameters which are 0.611 kPa, 17.502, and 240.97 °C (Campbell and Norman, 1998).

SWC data were converted to soil moisture deficit (SMD, dimensionless), defined as:

$$\text{SMD} = \frac{\text{SWC}_{max} - \text{SWC}}{\text{SWC}_{max} - \text{SWC}_{min}} \tag{2}$$

where SWC_{max} and SWC_{min} are the maximum and minimum values of SWC during the study period. SWC_{max} (0.49) occurred on 18 July 2005, while SWC_{min} (0.11) occurred on 26 December 2005.

2.2 Projected canopy area, leaf area index and sapwood area

Sapwood area (A_s), projected canopy area (A_c), and leaf area index (LAI) are key parameters to calculate stand transpiration and canopy stomatal conductance. A_c of

each tree in the plot was calculated as the area of an ellipse based on measurements of widest and narrowest canopy widths. LAI was randomly measured using a plant canopy analyzer (CID-110, CID COR., USA) at dawn, dusk or under cloudy conditions every month at 20 sampling sites. A_s of each tree in the plot was calculated based on strong allometric relationships between DBH and A_s ($A_s = 0.1930 \, (DBH)^{1.944}$. This relationship, established from measurements on 23 surrounding trees, has been reported in previous studies (Zhao et al., 2005b; Wang et al., 2012).

2.3 Sap flow measurement

Sap flux density (J_s, $g\,H_2O\,cm^{-2}\,s^{-1}$) was measured with self-made Granier-type sensors (Granier, 1987; Zhao et al., 2005b). One tree at the $< 15\,cm$ DBH class, four trees at the 15–20 cm DBH class, five trees at the 20–25 cm DBH class, two trees at the 25–30 cm DBH class, and two trees at the $> 30\,cm$ DBH class were selected for J_s measurement. For trees No. 1–No. 4, sensors were installed on the east, south, west, and north sides of the trunk, while for trees No. 5–No. 14, sensors were installed only on the north side. Sensors consisted of two 20-mm-long probes inserted into the xylem at breast height, with one placed 10 cm above the other. Each probe contained a copper-constantan thermocouple, and the upper probe was continuously heated with heating wire supplied with constant power. The temperature difference between two probes was taken every 30 s and recorded as 10 min means by a data logger (Delta-T Devices Ltd., Cambridge, UK). We selected the highest temperature difference between heated and unheated probes during times of zero flux (ΔT_m) as the baseline for each day (Granier, 1987; Phillips et al., 1997). Deviation from this baseline is used to estimate J_s (Granier, 1987).

2.4 Stand transpiration and canopy stomatal conductance

Whole-tree transpiration (E_t, $g\,s^{-1}$) was calculated as:

$$E_t = J_s \times A_s \tag{3}$$

Sapwood depth of sample trees measured with cores was close to 2 cm or somewhat larger, and *A. mangium* is a diffuse-porous species for which the radial variation in J_s is considered to be small (Phillips et al., 1996; Ma et al., 2008a). Therefore, radial variation in J_s was considered to be negligible in this study. Furthermore, the variation in J_s at different aspects was random for the studied trees (Ma et al., 2007). Hence, J_s at the north aspect was assumed to be representative of J_s of individual trees. For trees No. 1–No. 4, J_s was calculated as the mean of the values from four aspects, while for trees No. 5–No. 14, J_s was the value measured from north side.

The 47 trees within the stand were classified into 5 groups by DBH classes (Zhao et al., 2006) (Fig. 1). The average sap flux density of class i (J_{si}) was calculated as:

$$J_{si} = \sum \left(J_{sj} \times A_{sj} \right) / \sum A_{sj} \tag{4}$$

where J_{sj} is sap flux density of sample tree j, A_{sj} is sapwood area of sample tree j.

Sap flow measurements on 14 sample trees were extrapolated to stand level as in Zhao et al. (2005a):

$$E_s = \sum \left(J_{si} \times A_{si} \right) \tag{5}$$

where E_s is stand transpiration of *A. mangium* ($g\,s^{-1}$), and A_{si} is the sum of total sapwood area in class i.

E_s was converted to stand transpiration per unit of leaf area (E_L, $mm\,s^{-1}$) as in Zhao et al. (2005a):

$$E_L = \frac{E_s}{\text{LAI} \times A_G} \tag{6}$$

where LAI is the leaf area index ($1.95\,m^2\,m^{-2}$) and A_G is the total stand area ($640.5\,m^2$).

The *A. mangium* plantation has a low LAI, and thus an open, well-ventilated, aerodynamically rough canopy. Therefore, a strong coupling of canopy surface to the atmosphere can be assumed (Schäfer et al., 2000). Furthermore, since the diffusion of

CO$_2$ uptake of a mature *Acacia mangium* plantation

H. Wang et al.

the transpiration signal due to depletion and replenishment of stem-stored water is relatively small (Wang et al., 2012), the average sap flux in the sapwood multiplied by sapwood area: leaf area is equal to transpiration (E_L). Therefore, the mean canopy stomatal conductance (G_s, mmol $H_2O\,m^{-2}\,s^{-1}$) of the study stand can be calculated based on a simplified equation (Köstner et al., 1992):

$$G_s = \frac{E_L \times \rho \times G_V \times (T_a + 273)}{D} \tag{7}$$

where ρ is the density of water (998 kg m^{-3}), G_V is the universal gas constant adjusted for water vapor (0.462 m^3 kPa K^{-1} kg^{-1}), T_a is the air temperature (°C), and D is vapor pressure deficit (kPa). We used all data except for those that were excluded based on the following criteria: (1) data collected during and 2 h after rainfall were excluded to avoid the discrepancy between evaporation and tree transpiration (Granier et al., 2000); (2) data were excluded when global radiation, or vapour pressure deficit, or stand transpiration were too low ($< 5\%$ of the maximum value), because of the large relative uncertainties in computing G_s under these conditions (Granier et al., 2000); (3) data were excluded when $D < 0.6$ kPa for G_s estimation, to keep errors in G_s estimates to less than 10 % (Ewers and Oren, 2000).

Relationships between the ratio of canopy stomatal conductance to the maximum value (G_s/G_{smax}) and photosynthetically active radiation (PAR), vapour pressure deficit (D), and soil moisture deficit (SMD) were determined by boundary-line analysis and non-linear least squares, using the maximum of average G_s of 14 trees for different PAR (step width: 50 μmol m^{-2} s^{-1}), D (step width: 0.2 kPa), and SMD classes (step width: 0.1). The estimated boundary line by regression can be used to compare the responses among seasons, or years (Webb, 1972; Rico et al., 1996).

The response of G_s/G_{smax} to PAR was represented by the Michaelis-Menten quadratic hyperbolic function (Thornley and Johnson, 1990):

$$G_s/G_{smax} = \frac{PAR}{PAR + a} \tag{8}$$

where a is a fitted parameter, representing the value of global radiation which reduces canopy conductance to one half of its maximum value.

G_s was related to D within season and among years in order to estimate the sensitivity of stomata to D. The response function can be described as (Oren et al., 1999):

$$G_s = -m\ln(D) + b \tag{9}$$

where the parameter $-m$, the slope of the regression, quantifies stomatal sensitivity to D, and the parameter b, the intercept, is a reference G_s when $D = 1\,\text{kPa}$ ($\ln D = 0$). $-m$ and b were estimated using least squares regression with Sigma Plot 10.0 (Systat Software Inc., San Jose, California). The relationship between G_s and $\ln(D)$ provides a convenient benchmark for comparisons within season and among years. In addition, G_s/G_{smax} related to D obtains relative responses.

The quadratic response function between G_s/G_{smax} and SMD can be described as follows:

$$G_s/G_{smax} = y_0 + k_1 \times \text{SMD} + k_2 \times \text{SMD}^2 \tag{10}$$

where the parameters y_0, k_1 and k_2 were estimated using least squares regression with Sigma Plot 10.0 (Systat Software Inc., San Jose, California).

2.5 Carbon isotope measurements on leaf sap and air samples

10 mature leaves at different positions on the branches in the middle canopy were collected every 1 h and repeated twice from 06:00 to 17:00 on eight representative sunny days: 6 and 17 December 2006 (winter, dry season), 9 and 10 May 2007 (spring, wet season), 26 July 2007, 1 August 2007 (summer, wet season), 6 and 7 November 2007 (autumn, dry season). The leaf sap was forced out through the petiole, using a portable pressure chamber (PMS Instruments, Corvallis, Oregon, USA). Then, the leaf sap was sucked up with a micropipet and injected into a 10 mL vial. The samples were immediately frozen and stored in the freezer. Carbon isotope ratio of leaf sap samples

was determined on a gas chromatograph–isotope ratio mass spectrometer (Finnigan MAT 252, Finnigan, Bremen, Germany). Carbon isotopic compositions of soluble sugar, water-soluble organic matter in leaves and phloem sap have all been used as indicators of recent canopy photosynthate (Gessler et al., 2004; Hu et al., 2010; Rascher et al., 2010). There may be qualitative differences between using whole leaves and leaves sap to estimate carbon isotopic compositions, as the latter may integrate over a shorter time period than the former. Therefore, we used carbon isotopic compositions of leaf sap as an indicator of recent photosynthate.

Five air sampling points were situated at 10 m to 15 m above the ground in the canopy of *A. mangium* plantation. Air samples were collected twice per hour during the periods when leaf sap was collected. The air samples were collected with an electromagnetic pump and a plastic tube. The samples were then injected into pre-evacuated 500 mL gas sampling bags. At the same time, atmospheric CO_2 concentration was recorded by an infrared gas analyzer (IRGA) (LI-6262, Li-Cor Inc., Lincoln, NE, USA). CO_2 isotope ratio of air samples with cryogenic pretreatment was also determined on Finnigan MAT 252.

2.6 Canopy CO_2 uptake rate estimation

Canopy CO_2 uptake of *A. mangium* by combining sap flow and ^{13}C techniques, as proposed by Zhao et al. (2005a), was estimated as follows. Carbon isotopic compositions are specified as $\delta^{13}C$ values (Keeling, 1958):

$$\delta^{13}C = \left(R_p/R_s - 1\right) \times 1000 \tag{11}$$

where R_p is the abundance ratio of $^{13}C/^{12}C$ of the examined sample and R_s refers to the internationally recognized standard abundance ratio of $^{13}C/^{12}C$ (PDB).

In order to account for the influence of $^{13}C/^{12}C$ ratio in the air, isotope discrimination (Δ) is used to express the discrimination of plants against ^{13}C (Farquhar et al., 1982):

$$\Delta = \frac{\delta^{13}C_a - \delta^{13}C_p}{1 + \delta^{13}C_p} \quad (12)$$

where $\delta^{13}C_a$ and $\delta^{13}C_p$ stand for carbon isotope compositions in air and leaf sap. Δ is frequently used to derive intercellular CO_2 concentration (C_i), according the linear version by (Farquhar et al., 1982):

$$\Delta = a + (b - a) \times (C_i/C_a) \quad (13)$$

where a stands for the fractionation that occurs as CO_2 diffuses through stomates (4.4 ‰), b for fractionation during carboxylation (27.5 ‰), C_i for intercellular CO_2 concentration, and C_a for ambient CO_2 concentration.

The CO_2 uptake rate (F_{CO_2}, µmol $CO_2\,m^{-2}\,s^{-1}$) is then given by (Farquhar et al., 1982):

$$F_{CO_2} = g_{CO_2} \times C_a \times (1 - C_i/C_a) \quad (14)$$

where g_{CO_2} is stomatal conductance for CO_2.

Combining Eqs. (13) and (14), we then have:

$$F_{CO_2} = g_{CO_2} \times C_a \times \left(1 - \frac{\Delta - 4.4}{23.1}\right) \quad (15)$$

Stomatal conductance to water vapor (g_{H_2O}) can be converted to conductance for CO_2 by dividing the stomatal conductance by 1.6, giving:

$$F_{CO_2} = \frac{g_{H_2O}}{1.6} \times C_a \times \left(1 - \frac{\Delta - 4.4}{23.1}\right) \quad (16)$$

Equation (16) depicts a relationship linking F_{CO_2}, g_{H_2O}, C_a, and Δ at the leaf level. Subsequently this relationship could be scaled up to canopy level by incorporating G_s that is calculated with Eq. (7) using the sap flow-based stand transpiration.

G_s is expressed as a product of LAI and g_{H_2O}:

$$G_s = LAI \times g_{H_2O} \tag{17}$$

Thus, combining Eqs. (7), (14) and (17) leads to mean F_{CO_2} of our *A. mangium* stand:

$$\overline{F}_{CO_2} = \frac{E_L \times \rho \times G_V \times (T_a + 273)}{1.6 \times LAI \times D} \times C_a \times \left(1 - \frac{\Delta - 4.4}{23.1}\right) \tag{18}$$

The daily canopy CO_2 uptake for our mature *A. mangium* plantation is obtained based on the sap flow measurement-derived canopy stomatal conductance and seasonally integrated ^{13}C discrimination. The annual canopy CO_2 uptake is obtained by multiplying the daily means of canopy CO_2 uptake with the number of days. Daily and annual mean standard errors are also estimated. Subsequently, these values are compared with estimates from other methods, including gas exchange method, component carbon analyses, and modeling approaches.

2.7 Leaf gas exchange measurements

Leaf photosynthetic rate (P_n) and stomatal conductance (g_s) of 10 sun-exposed leaves and 10 shaded leaves from *A. mangium* trees at the study plot were measured with a portable gas exchange system (Li-Cor 6400, Li-Cor Inc., Lincoln, NE, USA). A frame platform was erected on the upper slope of the study plot so that the leaves within the canopy on the lower slope could be accessed. The measurements were taken on the same trees every hour from 06:00 to 19:00 (GMT + 08:00) on 6 and 17 December 2006 (winter, dry season), 9 and 10 May 2007 (spring, wet season), 26 July 2007, 1 August 2007 (summer, wet season), 6 and 7 November 2007 (autumn, dry season).

2.8 Statistics and sensitivity analysis

Statistical analyses were performed in SPSS 11.5 (SPSS Inc., Chicago, USA) and Sigmaplot 10.0 (Systat Software Inc., San Jose, CA). Independent *t*-tests were conducted to test whether there were statistically significant differences at $p < 0.05$ in C_a, C_i, C_i/C_a, $\delta^{13}C_p$, $\delta^{13}C_a$ and Δ between the wet and dry seasons, in C_i/C_a between the sunlit leaves and shaded leaves. Partial correlation analysis was used to determine the correlations between Δ and PAR, D, C_a, and G_s. Linear regression analyses between g_s and G_s, P_n and F_{CO_2} were performed. Non-linear regressions were performed on the correlation between G_s and D among seasons and years.

In order to quantify error propagation when modeling F_{CO_2} based on measurements of G_s, C_a and Δ, we applied a Monte Carlo method (Hollinger and Richardson, 2005; Hu et al., 2010) (Matlab R2008B, The Mathworks). This approach accounted for all known parameter uncertainties in calculating F_{CO_2}, including C_a and Δ (differences influenced by seasons), and G_s (differences influenced by tree size and seasonality in leaf area). For each selected day (8 days between December 2006 and November 2007), we modeled F_{CO_2} in an iterative manner (10 000 times) and randomly sampled from a range of uniformly distributed G_s, C_a and Δ values to calculate F_{CO_2}. Hence, we were able to estimate F_{CO_2} without the constraint of limited sampling frequency and could determine the sensitivity of the estimated F_{CO_2} to G_s, C_a and Δ. The range of the G_s (between 4.25 and 64.52 mmol m^{-2} s^{-1}), C_a (between 381.51 and 416.58 µmol mol^{-1}) and Δ (between 20.47 and 23.89 ‰) values used for constructing the pool of simulations was determined a priori. Because F_{CO_2} was modeled using both measurements of G_s, C_a and Δ, we used random values drawn from the same pool of F_{CO_2} values used in the Monte Carlo analysis, and examined the sensitivity of F_{CO_2} to G_s, C_a and Δ as independent variables. We plotted the linear regression relationship plus 95 % confidence intervals from this analysis for the data reported in Fig. 8.

Full Screen / Esc

Printer-friendly Version

Interactive Discussion

3   Results

3.1   Microclimate, leaf area index, and stand transpiration

Seasonal and inter-annual variability in vapor pressure deficit (D), photosynthetically active radiation (PAR), precipitation (P), soil water content (SWC), leaf area index (LAI), and stand transpiration (E_L) from 2004 to 2007 are shown in Fig. 2. E_L has clear seasonality, corresponding to D, PAR, and P seasonality, in contrast with the relatively small seasonal variation in LAI. The means of annual averages of D, SWC, and LAI were 0.46 kPa, 0.26 m^3 m^{-3}, and 1.95 m^2 m^{-2}, respectively. The means of annual totals of PAR, P, and E_L were 5752 mol m^{-2}, 1391 mm, and 220 mm, respectively. The inter-annual variability of D, PAR, SWC, and LAI was relatively small with coefficients of variation (CV) of 8.6 %, 3.0 %, 7.1 %, and 4.2 %. However, large inter-annual variability of P and E_L (CV 40.7 % and 26.7 %) was observed.

3.2   Diurnal and seasonal variability of C_a, C_i, C_i/C_a, δ_a, δ_p, Δ, and G_s

The diurnal ambient CO$_2$ concentration (C_a), intercellular CO$_2$ concentration (C_i), the ratio of the intercellular and ambient CO$_2$ concentrations (C_i/C_a), and carbon isotope compositions in leaf sap ($\delta^{13}C_p$) were higher in the morning and at dusk, but lower at noon (Fig. 3a, b, c, d, f), while isotope compositions in the canopy air ($\delta^{13}C_a$) and the photosynthetic ^{13}C discrimination (Δ) were lower in the early morning, gradually increased, and then slightly decreased from noon to dusk (Fig. 3e, g). The diurnal C_a, $\delta^{13}C_p$, $\delta^{13}C_a$, and Δ in the wet season fluctuated, while they were relatively flat in the dry season. The diurnal canopy stomatal conductance (G_s) increased rapidly just after sunrise, reached a maximum in the early or late morning, then decreased progressively, eventually declining to near zero values around sunset (Fig. 3h). G_s exhibited a narrow peak with a maximum around 100 mmol m^{-2} s^{-1} in the wet season, with a wider peak with a maximum around 50 mmol m^{-2} s^{-1} in the dry season. The

opening of stomata, as well as the time of maximum value (around 08:00), occurred earlier in the wet season than in the dry season (around 11:00).

The diurnal C_a, C_i, C_i/C_a, $\delta^{13}C_p$, $\delta^{13}C_a$, and Δ across wet and dry seasons were within the ranges of 366 to 451 $\mu mol\,mol^{-1}$, 243 to 373 $\mu mol\,mol^{-1}$, 0.63 to 0.94, -34.5 to $-26.6\,\permil$, -11.6 to $-7.0\,\permil$, and 17.6 to 26.3 $\permil$, respectively. CVs of diurnal C_a, C_i, C_i/C_a, $\delta^{13}C_p$, $\delta^{13}C_a$, and Δ were below 6.1 %, 16.0 %, 13.2 %, 7.9 %, 15.1 %, and 12.4 %, respectively. Because of the lack of strong variability in diurnal Δ values, the average Δ value was used in subsequent calculations of F_{CO_2} for the whole season. Further, values of diurnal C_i/C_a for sunlit leaves ranged between 0.55 and 0.94, while those of shaded leaves ranged between 0.68 and 0.95. Mean daily C_i/C_a value of 0.76 for sunlit leaves was significantly lower than that of 0.83 for shaded leaves ($p = 0.001$).

At the seasonal scale, the daily means of C_a, C_i, C_i/C_a, $\delta^{13}C_p$, $\delta^{13}C_a$, and Δ were 399 vs. 387 $\mu mol\,mol^{-1}$, 308 vs. 312 $\mu mol\,mol^{-1}$, 0.81 vs. 0.78, -31.4 vs. $-30.8\,\permil$, -9.6 vs. $-8.9\,\permil$, and 22.5 vs. 22.5 $\permil$ in the wet season and dry season. However, there were no significant differences in C_a, C_i, C_i/C_a, $\delta^{13}C_p$, $\delta^{13}C_a$, and Δ between the two seasons ($p = 0.212$, $p = 0.781$, $p = 0.238$, $p = 0.420$, $p = 0.118$, $p = 0.988$). CVs of seasonal C_a, C_i, C_i/C_a, $\delta^{13}C_p$, $\delta^{13}C_a$, and Δ were below 5.1 %, 5.0 %, 3.3 %, 5.1 %, 14.4 %, and 9.8 %, respectively.

Hourly Δ was negatively correlated with C_a ($r = -0.549$, $p < 0.001$) in the wet season, negatively correlated with PAR ($r = -0.425$, $p = 0.002$) and positively correlated with G_s ($r = 0.464$, $p < 0.001$) in the dry season, and positively correlated with D ($r = 0.250$, $p = 0.009$) over the entire year (Table 2). Boundary-line response curves using 10 min values of G_s and PAR, D, and SMD were created to determine the G_s response patterns in both the wet and dry seasons (Fig. 4). G_s in relation to PAR is shown in Fig. 4a–h. G_s increased with PAR, and appeared to be light-saturated at 400 and 200 $\mu mol\,m^{-2}\,s^{-1}$ in the wet season and dry season, respectively. However, all the regressions between G_s and PAR were insignificant. G_s in relation to D is shown in Fig. 4i–p. G_s decreased exponentially from D values of 0.6 and 0.8 kPa in the wet

season and dry season, respectively. Nearly all the regressions between G_s and D were significant ($p < 0.0001$), with R^2 ranging from 0.60 to 0.99. Stomatal sensitivity (m) was greater in the wet season than that in the dry season (Table 3). m increased linearly with reference canopy stomatal conductance (G_{sref}) (slope = 0.70, $R^2 = 0.96$, $n = 8$). G_s in relation to SMD is shown in Fig. 4q–t. G_s decreased as SMD increased in July in 2005 and 2006. However, no significant relationships between G_s and SMD were observed across entire years (ex. Tree No. 3 in year 2005 $p = 0.097$, Tree No. 4 in year 2005 $p = 0.064$).

3.3 Canopy CO$_2$ uptake rate of mature *A. mangium* plantation

Canopy CO$_2$ uptake rate (F_{CO_2}) varied diurnally (Fig. 5a). In the wet season, F_{CO_2} peaked around 09:00, with a maximum of $7.3\,\mu mol\,m^{-2}\,s^{-1}$. In the dry season, the diurnal pattern of F_{CO_2} was more symmetrical and smoother, reaching a maximum of $3.9\,\mu mol\,m^{-2}\,s^{-1}$ around 11:00. Based on daily F_{CO_2}, monthly, seasonal, and inter-annual F_{CO_2} were calculated. Maximum monthly F_{CO_2} occurred in July ($155\,g\,C\,m^{-2}$), May ($98\,g\,C\,m^{-2}$), July ($129\,g\,C\,m^{-2}$), and August ($117\,g\,C\,m^{-2}$) in 2004, 2005, 2006 and 2007, respectively (Fig. 5b). F_{CO_2} of the *A. mangium* stand in the wet season ($522\,g\,C\,m^{-2}$) was considerably higher than that in the dry season ($255\,g\,C\,m^{-2}$) (Fig. 5c). Annual F_{CO_2} was 820, 564, 895 and $828\,g\,C\,m^{-2}$ in 2004, 2005, 2006 and 2007, respectively. F_{CO_2} in the wet season contributed 72, 71, 66, and 61 % of the total annual CO$_2$ uptake (Fig. 5d). Across years 2004, 2005, 2006 and 2007, the daily and annual means of canopy CO$_2$ uptake for mature *A. mangium* plantation was $2.13 \pm 0.40\,g\,C\,m^{-2}\,day^{-1}$ and $776.89 \pm 145.76\,g\,C\,m^{-2}$, respectively. For comparison, the gross primary production (GPP) of forests in different climate zones, using several different methods, was summarized in Table 4. GPP in tropical forests ($8.35 \pm 0.23\,g\,C\,m^{-2}\,day^{-1}$) was significantly higher than that in sub-tropical forests ($5.38 \pm 0.46\,g\,C\,m^{-2}\,day^{-1}$, $p < 0.001$), and temperate forests ($2.85 \pm 0.45\,g\,C\,m^{-2}\,day^{-1}$, $p < 0.001$).

Diurnal leaf stomatal conductance (g_s), net photosynthesis (P_n) of *A. mangium* obtained through gas exchange measurements reached its peak around 09:00 in the wet season, and around 11:00 in the dry season (Fig. 6). The diurnal means of g_s in all leaves, sunlit leaves, and shaded leaves were 136.40, 129.42, and 144.34 mmol m^{-2} s^{-1} in the wet season, and 58.65, 56.74, and 60.42 mmol m^{-2} s^{-1} in the dry season. The diurnal means of P_n in all leaves, sunlit leaves, and shaded leaves were 3.42, 3.93, and 2.84 µmol m^{-2} s^{-1} in the wet season, and 1.85, 2.17, and 1.34 µmol m^{-2} s^{-1} in the dry season. Notably, CVs were high (ranging mostly from 40 % to 60 %) for g_s, and P_n. Further, the diurnal means of G_s and F_{CO_2} in all leaves were 56.70 mmol m^{-2} s^{-1} and 2.78 µmol m^{-2} s^{-1} in the wet season, 28.81 mmol m^{-2} s^{-1} and 1.32 µmol m^{-2} s^{-1} in the dry season. As shown in Fig. 6, values of both G_s and F_{CO_2} were lower than those of g_s, and of P_n, with regression coefficients of determination (R^2) of 0.58 and 0.19 in the wet season, 0.70 and 0.65 in the dry season, and 0.44 and 0.35 in all seasons respectively (Fig. 7).

3.4 Canopy CO_2 uptake rate sensitivity analysis

We examined the sensitivity of F_{CO_2} to changes in G_s, C_a and Δ between December 2006 and November 2007 (Table 5; Fig. 8). The positive correlation between G_s and F_{CO_2} was significant, and the R^2 value was high ($R^2 = 0.8263$; $p < 0.0001$). Although there were significant correlations between C_a and F_{CO_2} ($p = 0.0001$) and Δ and F_{CO_2} ($p < 0.0001$), the R^2 values were very low ($R^2 = 0.0016$ and $R^2 = 0.1348$, respectively).

4 Discussion

4.1 The theoretical basis for estimating canopy CO$_2$ uptake

Hu et al. (2010) used the Farquhar et al. (1989) model to relate δ^{13}C of needle sugars to C_i/C_a, calculate WUE using observations of D, and then isolate whole-tree carbon assimilation through multiplication with transpiration obtained from observations of xylem sap flux. However, the results are subject to the influence of D, even if this approach has good representation of sampling and is convenient to practice (Zhao et al., 2005a). Herein, the relation between Δ and C_i/C_a raised by Farquhar et al. (1982) is integrated with that between F_{CO_2} and stomatal conductance for CO$_2$, so that we get a new relationship linking Δ, F_{CO_2} and G_s, rather than that between Δ and E. Thus eliminating the influence of D on E (Zhao et al., 2005a). This sample approach, which can be used in heterogeneous and mountainous areas, is advantageous for its continuity and high accuracy.

4.2 Temporal patterns of canopy CO$_2$ uptake and its dependence on environment and stomata

Canopy CO$_2$ uptake rate (F_{CO_2}) varied diurnally (Fig. 5). The sharp peak in photosynthesis in early morning periods during the wet season may be due to higher G_s and C_a, as well as lower Δ during this period. During the wet season G_s peaked around 08:00 and then rapidly dropped for the rest of the day (Fig. 3h). This diurnal pattern was similar to that of canopy conductance on well-watered 9 yr-old Sultana grapevines (Lu et al., 2003), native forest composed by *Lomatia hirsuta*, *Schinus patagonicus*, *Nothofagus antarctica* and *Diostea juncea* (Fernandez et al., 2009), and pristine *Nothofagus* forest (Köstner et al., 1992). Usually under drier conditions, stomata will open in the morning, then close around midday as D increases; here the pattern seems quite different, Because the trees are on a steep slope, it may be that the G_s reflected the changes in illumination (total amount and timing). Accounting for nocturnal sap flux caused by the

recharge of water to trunks and branches, as well as nocturnal transpiration, is a vital step for accurately estimating canopy transpiration, and thereby canopy CO_2 uptake. A greater allocation of nighttime sap flow to the refilling of depleted water storage has been found in the same *A. mangium* trees (Wang et al., 2012). In view of the obvi-
5 ous nocturnal water recharge, we used the 24 h diurnal sap flux to accurately estimate canopy CO_2 uptake.

Strong seasonality in F_{CO_2} of *A. mangium* was observed (Fig. 5). Based on this, we related F_{CO_2} to the seasonally changing environmental variables. Higher F_{CO_2} in the wet season coincided with the season of rapid growth, ample supply of water, and strong
10 solar radiation, the typical environment of subtropical ecosystems (Figs. 2, 5). Notably, in the dry season, water supply did not match that of heat load at the study site, since P and SWC were relatively low, while PAR and T_a were still sufficient. This conflict may affect tree physiological activities in that higher heat load can meet the demands of photosynthesis, but may induce water stress in *A. mangium* in the dry season. Further,
15 lower annual F_{CO_2} and maximum monthly F_{CO_2} in May in 2005 were due to the frequent rainfall occurred in June and July.

Canopy stomatal conductance is a critical factor regulating F_{CO_2} of *A. mangium*. Estimates of canopy conductance from the Penman–Monteith formula were very close to those obtained with the simplified equation by Köstner et al. (1992) (Ma, 2008), as
20 would be expected given that the Köstner et al. (1992) equation is based on Penman–Monteith. The diurnal pattern of F_{CO_2} was similar to that of G_s (Figs. 3, 5). G_s was mainly influenced by D and PAR (Fig. 4). When D was lower than 0.6 kPa, PAR was the main driver of G_s, because it induced stomatal opening. When D approached 0.6 kPa and beyond, D became the dominant factor. The increase of D led to a decrease in G_s
25 despite the increase in PAR, because the hydraulic system needed to be protected. High D led to varying degrees of decline in G_s (Table 3), and thus the corresponding reduction in F_{CO_2}. The slope of this linear function between stomatal sensitivity (m) and reference canopy stomatal conductance (G_{sref}) was consistent with the shallower slope of approximately 0.60 observed for the mesic species in Oren et al. (1999). Inconsistent

Full Screen / Esc

Printer-friendly Version

Interactive Discussion

with our results, G_s stayed high at low D and thus allowed high H_2O flux in a planted exotic species (*Pseudotsuga menziesii*) in South America (Fernandez et al., 2009).

4.3 Comparison with estimates from gas exchange measurements

Comparisons between gas exchange measurements and sap flux/stable isotope method (SF/SI) results were conducted in this study (Figs. 6, 7). With regard to the patterns, the diurnal dynamics of gas exchange results agreed well with that of SF/SI results. Better agreement between F_{CO_2} and P_n in the dry season was likely due to the fact that the lower leaf area index in the dry season would tend to minimize the effects of leaf shading, which can diminish conductance in lower-canopy leaves. As for the values, F_{CO_2} from SF/SI were 27.0 % lower than P_n from gas exchange measurements. The diurnal C_i/C_a from gas exchange measurements and stable isotope values ranged from 0.63 to 0.94 and from 0.57 to 0.95, respectively. The seasonal C_i/C_a from gas exchange measurements and stable isotope values in the wet season (0.80, 0.78), dry season (0.78, 0.78), whole year (0.79, 0.78) were also matched well. Thus, the differences in F_{CO_2} and P_n resulted mainly from differences in stomatal conductance. Further, the differences may also be attributed to high variation in gas exchange results that were variable by leaf position and age, and thus any one measurement was not representative of the entire canopy, and variability of the average response was high. Given that F_{CO_2} was calculated based on Δ and C_i/C_a averaged across a variety of age and light classes, this source of variation was reduced for the SF/SI results. The analysis of the differences between the gas exchange and SF/SI results heightened the advantages of the latter method.

4.4 Comparison with estimates from other approaches for estimating F_{CO_2}

Most of the differences in the gross primary production (GPP) of forests in various climate zones were related to climate (Table 4). Our estimate of canopy CO_2 uptake for a mature *A. mangium* plantation ($2.13 \pm 0.40\,\mathrm{g\,C\,m^{-2}\,day^{-1}}$, Fig. 5) approached the

Title Page

Abstract | Introduction

Conclusions | References

Tables | Figures

|◄ | ►|

◄ | ►

Back | Close

Full Screen / Esc

Printer-friendly Version

Interactive Discussion

lower range of values for subtropical mixed forest (Gebremichael and Barros, 2006; Gu et al., 2006). Our lower estimates of GPP may be due to the lower mean canopy stomatal conductance (0.135 cm s^{-1} vs. 0.726 cm s^{-1}, 0.25 cm s^{-1}), higher C_i/C_a (0.76 to 0.84), greater tree height (17.8 m vs. 10.8 m, 2 m), and lower LAI (1.95 m^2 m^{-2} vs.

5　3.20 m^2 m^{-2}, 3.77 m^2 m^{-2}), compared to other subtropical mixed forests (Ma, 2008; Gebremichael and Barros, 2006; Gu et al., 2006). Our C_i/C_a ratio varied from 0.76 to 0.84, which was higher than the ranges found in cottonwoods in a riparian woodland (0.75–0.78) (Letts et al., 2008), in 13-yr-old loblolly pine (*Pinus taeda*) trees (0.45–0.80) (Maier et al., 2002), and in nine well-watered conifer species (0.57–0.68) (Brodribb,

10　1996), leading to a decline in photosynthetic capacity in *A. mangium*. Relatively high C_i/C_a ratios have also been found in a Canarian laurel forest tree species (*Laurus azorica*) (0.67–0.95) (González-Rodríguez et al., 2001). The canopy stomatal conductance of individual tree decreases with tree height (Schäfer et al., 2000), while the lower LAI might lead to higher conductance and more control by stomatal conductance, since

15　there is less shading (Granier et al., 2000).

　　Notably, our estimate of canopy CO$_2$ uptake for 20 yr-old *A. mangium* stand was much lower than that for 4–6 yr-old *A. mangium* (8.77 g C m^{-2} day^{-1}) in São Paulo, Brazil (Nouvellon et al., 2012). Our lower estimates of GPP may be partly explained by an age-related decline in photosynthesis. Further, we compared methods for quan-

20　tifying GPP constrained by water use measurements. Our estimates were comparable with those of spruce (2.66 g C m^{-2} day^{-1}) and mixed forest (0.94 g C m^{-2} day^{-1}) also using the sap flow based approach (Köstner et al., 2008; Hu et al., 2010), but lower than values determined by satellite-based modeling or component carbon analysis (Table 4). These differences suggest the necessity of measuring species-specific fluxes in

25　assessing CO$_2$ uptake.

4.5 Sensitivity analysis

Through our sensitivity analysis using a Monte Carlo approach, we were able to obtain many more combinations of G_s, C_a and Δ obtained from our limited 8 day samplings. We found that the dynamics in the estimates of F_{CO_2} were mainly driven by dynamics in G_s, compared with C_a and Δ (Fig. 8). Hu et al. (2010) also demonstrated that the calculation of canopy photosynthesis was much more sensitive to transpiration rate than to δ^{13}C values. In our study, covariance between G_s and F_{CO_2} is forced on the fact that CO_2 is assimilated through the stomatal pores. In our model shown in Eq. (15), the proportioning coefficient between G_s and F_{CO_2} is Δ, which is ultimately dependent on the scaling between G_s and F_{CO_2}. Therefore, we get a mechanistic relationship linking Δ, G_s and F_{CO_2}. Variation in Δ between seasons is insignificant ($p = 0.988$), compared with variation in G_s, since Δ is mathematically constrained as the ratio of two covarying fluxes, and partly because stomata function in a way that optimizes G_s and F_{CO_2} toward conserved values in response to environmental changes (Wong et al., 1979). Further, C_i/C_a is a very useful parameter to model F_{CO_2}. Seasonally constant C_i/C_a values have reported from a wide range of field experiments (Norman, 1982; Ellsworth, 1999; Letts et al., 2008). A constant C_i/C_a, which is most parsimonious in terms of number of input parameters, yields results that are comparable or better than more elaborate models for predicting assimilation (Katul et al., 2000). In our study, no significant seasonal variation was observed in C_i/C_a (Fig. 3, $p > 0.05$), although variation in diurnal C_i/C_a between the sunlit leaves and shaded leaves was found. Therefore, we argue that an acceptable estimate of F_{CO_2} of a subtropical mature *A. mangium* plantation was obtained by using seasonally integrated/constant C_i/C_a values.

The relatively high sensitivity of the model to G_s, and low sensitivity to C_a and Δ also indicate that one source of potential error that may be significant in the model is the uncertainty in estimating G_s. Error in G_s can occur in measurements of sap flow and tree size. We accounted for errors in G_s using the Monte Carlo approach, where we generated 99 % intervals for our modeled F_{CO_2} values. No values fell outside our

99 % confidence intervals, suggesting that most errors of G_s are accounted for in our modeled F_{CO_2} rates.

5 Conclusions

Our study demonstrated that combining sap flow measurement and stable isotope dis-
crimination provided a simple and accurate way to estimate canopy scale photosyn-
thesis. We concluded that mature *A. mangium* exhibited obvious diurnal, seasonal,
annual, and inter-annual changes in canopy CO_2 uptake (F_{CO_2}). The temporal changes
of F_{CO_2} were attributed to the responsiveness of G_s to environmental factors. Large
diurnal, seasonal, and inter-annual variability in F_{CO_2} with low variability of diurnal and
seasonal C_a and Δ suggested that canopy photosynthetic patterns mimicked those of
water flux to a large degree. Our lower estimate of F_{CO_2} for mature *A. mangium* planta-
tion was likely related to the lower mean canopy stomatal conductance, higher C_i/C_a,
greater tree height, and aging. Compared with results from satellite-based modeling
or component carbon analyses, our estimate may suggest the necessity to consider
species-specific fluxes in CO_2 assessment.

References

Baldocchi, D., Valentini, R., Running, S., Oechel, W., and Dahlman, R.: Strategies for measuring and modelling carbon dioxide and water vapour fluxes over terrestrial ecosystems, Glob. Change Biol., 2, 159–168, doi:10.1111/j.1365-2486.1996.tb00069.x, 1996.

**CO$_2$ uptake of
a mature *Acacia
mangium* plantation**

H. Wang et al.

Title Page

Abstract   Introduction

Conclusions   References

Tables   Figures

|◄   ►|

◄   ►

Back   Close

Full Screen / Esc

Printer-friendly Version

Interactive Discussion

Brodribb, T.: Dynamics of changing intercellular CO_2 concentration (ci) during drought and determination of minimum functional ci, Plant Physiol., 111, 179–185, doi:10.1104/pp.111.1.179, 1996.

Campbell, G. S. and Norman, J. M.: An Introduction to Environmental Biophysics. Springer-Verlag, New York, 36–51, 1998.

Catovsky, S., Holbrook, N. M., and Bazzaz, F. A.: Coupling whole-tree transpiration and canopy photosynthesis in coniferous and broad-leaved tree species, Can. J. Forest Res., 32, 295–309, doi:10.1139/x01-199, 2002.

Ciais, P., Tans, P. P., Trolier, M., White, J. W. C., and Francey, R. J.: A large Northern Hemisphere terrestrial CO_2 sink indicated by the $^{13}C/^{12}C$ ratio of atmospheric CO_2, Science, 269, 1098–1102, doi:10.1126/science.269.5227.1098, 1995.

Cole, T. G., Yost, R. S., Kablan, R., and Olsen, T.: Growth potential of twelve *Acacia* species on acid soils in Hawaii, Forest Ecol. Manag., 80, 175–186, doi:10.1016/0378-1127(95)03610-5, 1996.

Dawson, T. E., Mambelli, S., Plamboeck, A. H., Templer, P. H., and Tu, K. P.: Stable isotope in plant ecology, Annu. Rev. Ecol. S., 33, 507–559, doi:10.1146/annurev.ecolsys.33.020602.095451, 2002.

Ewers, B. E. and Oren, R.: Analyses of assumptions and errors in the calculation of stomatal conductance from sap flux measurements, Tree Physiol., 20, 579–589, doi:10.1093/treephys/20.9.579, 2000.

Fang, J. Y. and Chen, A. P.: Dynamic forest biomass carbon pools in China and their significance, Acta Bot. Sin., 43, 967–973, 2001 (in Chinese with English abstract).

Farquhar, G. D., Caemmerer, S., and Berry, J. A.: A biochemical model of photosynthetic CO_2 assimilation in leaves of C_3 species, Planta, 149, 78–90, doi:10.1007/bf00386231, 1980.

Farquhar, G. D., O'Leary, M., and Berry, J.: On the relationship between carbon isotope discrimination and the intercellular carbon dioxide concentration in leaves, Funct. Plant Biol., 9, 121–137, doi:10.1071/PP9820121,1982.

Farquhar, G. D., Ehleringer, J. R., and Hubick, K. T.: Carbon isotope discrimination and photosynthesis. Annu. Rev. Plant Physiol. Plant Mol. Biol., 40, 503–537, doi:10.1146/annurev.pp.40.060189.002443, 1989.

Fernandez, M. E., Gyenge, J., and Schlichter, T.: Water flux and canopy conductance of natural versus planted forests in Patagonia, South America, Trees-Struct. Funct., 23, 415–427, doi:10.1007/s00468-008-0291-y, 2009.

Gebremichael, M. and Barros, A. P.: Evaluation of MODIS Gross Primary Productivity (GPP) in tropical monsoon regions, Remote Sens. Environ., 100, 150–166, doi:10.1016/j.rse.2005.10.009, 2006.

Gessler, A., Rennenberg, H., and Keitel, C.: Stable isotope composition of organic compounds transported in the phloem of European beech – evaluation of different methods of phloem sap collection and assessment of gradients in carbon isotope composition during leaf-to-stem transport, Plant Biol., 6, 721–729, doi:10.1055/s-2004-830350, 2004.

González-Rodríguez, A. M., Morales, D., and Jiménez, M. S.: Gas exchange characteristics of a Canarian laurel forest tree species (*Laurus azorica*) in relation to environmental conditions and leaf canopy position, Tree Physiol., 21, 1039–1045, doi:10.1093/treephys/21.14.1039, 2001.

Granier, A.: Evaluation of transpiration in a Douglas-fir stand by means of sap flow measurements, Tree Physiol., 3, 309–320, doi:10.1093/treephys/3.4.309, 1987.

Granier, A., Loustau, D., and Bréda, N.: A generic model of forest canopy conductance dependent on climate, soil water availability and leaf area index, Ann. For. Sci., 57, 755–765, doi:10.1051/forest:2000158, 2000.

Gu, F., Cao, M., Wen, X., Liu, Y., and Tao, B.: A comparison between simulated and measured CO_2 and water flux in a subtropical coniferous forest, Sci. China Ser. D, 49, 241–251, doi:10.1007/s11430-006-8241-2, 2006.

Hollinger, D. Y. and Richardson, A. D.: Uncertainty in eddy covariance measurements and its application to physiological models, Tree Physiol., 25, 873–885, doi:10.1093/treephys/25.7.873, 2005.

Hu, J., Moore, D. J. P., Riveros-Iregui, D. A., Burns, S. P., and Monson, R. K.: Modeling whole-tree carbon assimilation rate using observed transpiration rates and needle sugar carbon isotope ratios, New Phytol., 185, 1000–1015, doi:10.1111/j.1469-8137.2009.03154.x, 2010.

Janssens, I. A., Lankreijer, H., Matteucci, G., Kowalski, A. S., Buchmann, N., Epron, D., Pilegaard, K., Kutsch, W., Longdoz, B., Grünwald, T., Montagnani, L., Dore, S., Rebmann, C., Moors, E. J., Grelle, A., Rannik, Ü., Morgenstern, K., Oltchev, S., Clement, R., Guðmundsson, J., Minerbi, S., Berbigier, P., Ibrom, A., Moncrieff, J., Aubinet, M., Bernhofer, C., Jensen, N. O., Vesala, T., Granier, A., Schulze, E. D., Lindroth, A., Dolman, A. J., Jarvis, P. G., Ceulemans, R., and Valentini, R.: Productivity overshadows temperature in determining soil and ecosystem respiration across European forests, Glob. Change Biol., 7, 269–278, doi:10.1046/j.1365-2486.2001.00412.x, 2001.

CO_2 uptake of a mature *Acacia mangium* plantation

H. Wang et al.

Title Page

Abstract | Introduction

Conclusions | References

Tables | Figures

|◄ | ►|

◄ | ►

Back | Close

Full Screen / Esc

Printer-friendly Version

Interactive Discussion

Katul, G. G., Ellsworth, D. S., and Lai, C. T.: Modelling assimilation and intercellular CO_2 from measured conductance: a synthesis of approaches, Plant Cell Environ., 23, 1313–1328, doi:10.1046/j.1365-3040.2000.00641.x, 2000.

Keeling, C. D.: The concentration and isotopic abundances of atmospheric carbon dioxide in rural areas, Geochim. Cosmochim. Acta, 13, 322–334, doi:10.1016/0016-7037(58)90033-4, 1958.

Kim, H., Oren, R., and Hinckley, T. M.: Actual and potential transpiration and carbon assimilation in an irrigated poplar plantation, Tree Physiol., 28, 559–577, doi:10.1093/treephys/28.4.559, 2008.

Köstner, B. M. M., Schulze, E. D., Kelliher, F. M., Hollinger, D. Y., Byers, J. N., Hunt, J. E., Mc-Seveny, T. M., Meserth, R., and Weir, P. L.: Transpiration and canopy conductance in a pristine broad-leaved forest of *Nothofagus*: an analysis of xylem sap flow and eddy correlation measurements, Oecologia, 91, 350–359, doi:10.1007/BF00317623, 1992.

Köstner, B., Matyssek, R., Heilmeier, H., Clausnitzer, F., Nunn, A. J., and Wieser, G.: Sap flow measurements as a basis for assessing trace-gas exchange of trees, Flora, 203, 14–33, doi:10.1016/j.flora.2007.09.001, 2008.

Letts, M. G., Phelan, C. A., Johnson, D. R. E., and Rood, S. B.: Seasonal photosynthetic gas exchange and leaf reflectance characteristics of male and female cottonwoods in a riparian woodland, Tree Physiol., 28, 1037–1048, doi:10.1093/treephys/28.7.1037, 2008.

Lu, P., Yunusa, I. A. M., Walker, R. R., and Müller, W. J.: Regulation of canopy conductance and transpiration and their modelling in irrigated grapevines, Funct. Plant Biol., 30, 689–698, doi:10.1093/treephys/20.10.683, 2003.

Ma, L., Rao, X. Q., Zhao, P., Lu, P., Cai, X. A., and Zeng, X. P.: Diurnal and seasonal changes in whole-tree transpiration of *Acacia mangium*, J. Beijing Forestry Univ., 29, 67–73, 2007 (in Chinese with English abstract).

Ma, L.: Transpiration of *Acacia mangium* and it's coupling to environmental factors at different temporal and spatial scales, Graduate School of the Chinese Academy of Sciences, Beijing, China, 2008 (in Chinese with English abstract).

Ma, L., Lu, P., Zhao, P., Rao, X. Q., Cai, X. A., and Zeng, X. P.: Diurnal, daily, seasonal and annual patterns of sap-flux-scaled transpiration from an *Acacia mangium* plantation in South China, Ann. For. Sci., 65, 402p1–402p9, doi:10.1051/forest:2008013, 2008a.

Ma, Z., Liu, Q., Wang, H., Li, X., Zeng, H., and Xu, W.: Observation and modeling of NPP for *Pinus elliottii* plantation in subtropical China, Sci. China Ser. D, 51, 955–965, doi:10.1007/s11430-008-0075-7, 2008b.

Maier, C. A., Johnsen, K. H., Butnor, J., Kress, L. W., and Anderson, P. H.: Branch growth and gas exchange in 13-year-old loblolly pine (*Pinus taeda*) trees in response to elevated carbon dioxide concentration and fertilization, Tree Physiol., 22, 1093–1106, doi:10.1093/treephys/22.15-16.1093, 2002

Malhi, Y., Nobre, A. D., Grace, J., Kruijt, B., Pereira, M. G. P., Culf, A., and Scott, S.: Carbon dioxide transfer over a Central Amazonian rain forest, J. Geophys. Res., 103, 31593–31612, doi:10.1029/98jd02647, 1998.

Morén, A. S., Lindroth, A., and Grelle, A.: Water-use efficiency as a means of modelling net assimilation in boreal forests, Trees-Struct. Funct., 15, 67–74, doi:10.1007/s004680000078, 2001.

Norman, J. M.: Simulation of microclimates, in: Biometeorology and Integrated Pest Management, Academic Press, New York, 1982.

Nouvellon, Y., Laclau, J., Epron, D., Le Maire, G., Bonnefond, J., Gonçalves, J. L. M., and Bouillet, J.: Production and carbon allocation in monocultures and mixed-species plantations of *Eucalyptus grandis* and *Acacia mangium* in Brazil, Tree Physiol., 32, 680–695, doi:10.1093/treephys/tps041, 2012.

Nowak, D. J., Stevens, J. C., Sisinni, S. M., and Luley, C. J.: Effects of urban tree management and species selection on atmospheric carbon dioxide, J. Arboricult., 28, 113–122, 2002.

Oren, R., Sperry, J. S., Katul, G. G., Pataki, D. E., Ewers, B. E., Phillips, N., and Schäfer, K. V. R.: Survey and synthesis of intra- and interspecific variation in stomatal sensitivity to vapour pressure deficit, Plant Cell Environ., 22, 1515–1526, doi:10.1046/j.1365-3040.1999.00513.x, 1999.

Oren, R., Ellsworth, D. S., Johnsen, K. H., Phillips, N., Ewers, B. E., Maier, C., Schäfer, K. V. R., McCarthy, H., Hendrey, G., McNulty, S. G., and Katul, G. G.: Soil fertility limits carbon sequestration by forest ecosystems in a CO_2-enriched atmosphere, Nature, 411, 469–472, doi:10.1038/35078064, 2001.

Peng, S. L.: Study and Application of Restoration Ecology in Tropical and Subtropical China, Science Press, Beijing, 2003.

CO$_2$ uptake of a mature *Acacia mangium* plantation

H. Wang et al.

Phillips, N., Oren, R., and Zimmermann, R.: Radial patterns of xylem sap flow in non-, diffuse- and ring-porous tree species, Plant Cell Environ., 19, 983–990, doi:10.1111/j.1365-3040.1996.tb00463.x, 1996.

Phillips, N., Nagchaudhuri, A., Oren, R., and Katul, G.: Time constant for water transport in loblolly pine trees estimated from time series of evaporative demand and stem sapflow, Trees-Struct. Funct., 11, 412–419, doi:10.1007/s004680050102, 1997.

Rascher, K. G., Máguas, C., and Werner, C.: On the use of phloem sap δ^{13}C as an indicator of canopy carbon discrimination, Tree Physiol., 30, 1499–1514, doi:10.1093/treephys/tpq092, 2010.

Rico, M., Gallego, H. A., Moreno, G., and Santa Regina, I.: Stomatal response of *Quercus pyrenaica* Willd to environmental factors in two sites differing in their annual rainfall (Sierra de Gata, Spain), Ann. For. Sci., 53, 221–234, doi:10.1051/forest:19960205, 1996.

Schäfer, K. V. R., Oren, R., and Tenhunen, J. D.: The effect of tree height on crown level stomatal conductance, Plant Cell Environ., 23, 365–375, doi:10.1046/j.1365-3040.2000.00553.x, 2000.

Schäfer, K. V. R., Oren, R., Ellsworth, D. S., Lai, C., Herrick, J. D., Finzi, A. C., Richter, D. D., and Katul, G. G.: Exposure to an enriched CO_2 atmosphere alters carbon assimilation and allocation in a pine forest ecosystem, Glob. Change Biol., 9, 1378–1400, doi:10.1046/j.1365-2486.2003.00662.x, 2003.

Schneider, S. H.: The changing climate, Sci. Am., 261, 70–79, 1989.

Thornley, J. H. M. and Johnson, I. R.: Plant and Crop Modelling, Clarendon Press, Oxford, 1990.

Wang, H., Zhao, P., Hölscher, D., Wang, Q., Lu, P., Cai, X. A., and Zeng, X. P.: Nighttime sap flow of *Acacia mangium* and its implications for nighttime transpiration and stem water storage, J. Plant Ecol., 5, 294–304, doi:10.1093/jpe/rtr025, 2012.

Waring, R. H., Landsberg, J. J., and Williams, M.: Net primary production of forests: a constant fraction of gross primary production?, Tree Physiol., 18, 129–134, doi:10.1093/treephys/18.2.129, 1998.

Webb, R. A.: Use of the boundary line in the analysis of biological data, J. Hortic. Sci., 47, 309–319, 1972.

Williams, M., Rastetter, E. B., Fernandes, D. N., Goulden, M. L., Shaver, G. R., and Johnson, L. C.: Prediction goss primary productivity in terrestrial ecosystems, Ecol. Appl., 7, 882–894, doi:10.1890/1051-0761(1997)007[0882:pgppit]2.0.co;2, 1997.

Title Page

Abstract | Introduction

Conclusions | References

Tables | Figures

|◄ | ►|

◄ | ►

Back | Close

Full Screen / Esc

Printer-friendly Version

Interactive Discussion

Wong, S. C., Cowan, I. R., and Farquhar, G. D.: Stomatal conductance correlates with photosynthetic capacity, Nature, 282, 424–426, doi:10.1038/282424a0, 1979.

Xiao, X., Zhang, Q., Saleska, S., Hutyra, L., De Camargo, P., Wofsy, S., Frolking, S., Boles, S., Keller, M., and Moore III, B.: Satellite-based modeling of gross primary production in a seasonally moist tropical evergreen forest, Remote Sens. Environ., 94, 105–122, doi:10.1016/j.rse.2004.08.015, 2005.

Yang, L., Liu, N., Ren, H., and Wang, J.: Facilitation by two exotic Acacia: *Acacia auriculiformis* and *Acacia mangium* as nurse plants in South China, Forest Ecol. Manag., 257, 1786–1793, doi:10.1016/j.foreco.2009.01.033, 2009.

Zhao, P., Lu, P., Ma, L., Sun, G. C., Rao, X. Q., Cai, X. A., and Zeng, X. P.: Combining sap flow measurement-based canopy stomatal conductance and ^{13}C discrimination to estimate forest carbon assimilation, Chinese Sci. Bul., 50, 2021–2027, 2005a.

Zhao, P., Rao, X. Q., Ma, L., Cai, X. A., and Zeng, X. P.: Application of Granier's sap flow system in water use of *Acacia mangium* forest, J. Trop. Subtrop. Bot. 13, 457–468, 2005b (in Chinese with English abstract).

Zhao, P., Rao, X. Q., Ma, L., Cai, X. A., and Zeng, X. P.: Sap flow-scaled transpiration and canopy stomatal conductance in an *Acacia mangium* forest, J. Plant Ecol. 30, 655–665, 2006 (in Chinese with English abstract).

Title Page

Abstract | Introduction

Conclusions | References

Tables | Figures

◀ | ▶

◀ | ▶

Back | Close

Full Screen / Esc

Printer-friendly Version

Interactive Discussion

Table 1. Tree height, diameter at breast height (DBH), projected canopy area (A_c), and sapwood area (A_s) of *A. mangium* trees used for sap flow measurements.

Tree no.	Height (m)	DBH (cm)	A_c (m^2)	A_s (m^2)
1	17.9	23.88	10.84	0.0137
2	19.3	29.29	17.37	0.0201
3	22.8	32.89	40.24	0.0248
4	19.5	37.51	47.71	0.0316
5	15.6	18.15	8.06	0.0083
6	14.5	17.19	8.37	0.0075
7	12.0	16.89	10.63	0.0072
8	19.5	23.88	8.55	0.0137
9	18.2	21.33	6.97	0.0111
10	18.7	25.47	9.66	0.0155
11	19.5	20.38	4.59	0.0102
12	20.0	20.7	15.54	0.0105
13	12.0	13.37	13.29	0.0047
14	19.5	18.15	5.51	0.0083

Table 2. Partial correlations between hourly Δ and photosynthetically active radiation (PAR), vapor pressure deficit (D), ambient CO$_2$ concentration (C_a), and canopy stomatal conductance (G_s).

Periods	Variables	Control variables	df	Δ Partial correlation
One year	PAR	D, C_a, G_s	107	−0.052
	D	PAR, C_a, G_s	107	0.250[a]
	C_a	PAR, D, G_s	107	0.016
	G_s	PAR, D, C_a	107	0.127
Wet season	PAR	D, C_a, G_s	51	0.030
	D	PAR, C_a, G_s	51	0.058
	C_a	PAR, D, G_s	51	−0.549[a]
	G_s	PAR, D, C_a	51	−0.198
Dry season	PAR	D, C_a, G_s	51	−0.425[a]
	D	PAR, C_a, G_s	51	0.136
	C_a	PAR, D, G_s	51	0.156
	G_s	PAR, D, C_a	51	0.464[a]

[a] indicates significant partial correlation at 0.01 level.

Table 3. Stomatal sensitivity to vapor pressure deficit (D) estimated as the slope of the relationship between canopy stomatal conductance and ln(D) (Oren et al., 1999), applied to those data in which G_s decreased exponentially with D.

Periods	Sensitivity (m)	$G_{sref}(b)$	m/b	Relative sensitivity	D threshold
Jul 2004	−114.56	162.03	−0.71	−0.40	0.60
Jul 2005	−48.27	75.25	−0.64	−0.35	0.60
Jul 2006	−71.67	113.48	−0.63	−0.26	0.60
Jul 2007	−86.52	146.65	−0.59	−0.30	0.60
Dec 2004	−16.11	34.33	−0.47	−0.40	0.60
Dec 2005	−13.36	36.70	−0.36	−0.31	0.80
Dec 2006	−56.15	79.48	−0.71	−0.69	0.60
Dec 2007	−69.50	120.20	−0.58	−0.53	0.80

Relative sensitivity was estimated using relative G_s values of each species instead of absolute values. D threshold is the value of leaf to air vapor pressure difference from which G_s begins to decrease in an exponential form. Reference canopy stomatal conductance (G_{sref}) is G_s at $D = 1$ kPa.

Table 4. Published estimates of gross primary production (GPP, $gCm^{-2}day^{-1}$), species, site information and methodology, in different climate zones.

Climate	Site (P mm/T_a °C)[1]	Dominate Species (Age)	Latitude/Longitude	Method	GPP	References
Tropical	Santarém, Brazil (1920/25.8)	Evergreen Forest	2°51′ S/54°58′ W	Satellite-based Model	7.97	Xiao et al. (2005)
	Manaus, Brazil (2200/-)	Tropical Rain Forest	2°35′ S/60°06′ W	Component Carbon Analyses	8.33	Malhi et al. (1998)
	São Paulo, Brazil (1280/21.3)	*Acacia mangium* (4–6)	23°02′ S/48°38′ W	Component Carbon Analyses	8.77	Nouvellon et al. (2012)
Subtropical	JiangXi, China	Mixed Forest[2]	26°44′ N/115°04′ E	CEVSA Model[3]	4.68	Gu et al. (2006)
		Mixed Forest[2]	26°44′ N/115°04′ E	Flux Measurements	4.41	Gu et al. (2006)
		Pinus elliottii	26°44′ N/115°04′ E	Biome-BGC Model	5.32	Ma et al. (2008b)
	Marsyandi, Nepal	Mixed Forest	28°21′ N/84°15′ E	MODIS_DAO	6.36	Gebremichael and Barros (2006)
				MODIS_Tower	3.59	Gebremichael and Barros (2006)
	New South Wales, Australia	*Pinus radiate* Plantations	35°21′ S/148°56′ E	Component Carbon Analyses	6.78	Waring et al. (1998)
	North Carolina, USA (1140/15.5)	*Pinus taeda*[4]	35°58′ N/79°05′ W	4C-A Model[5]	6.54	Schäfer et al. (2003)
Temperate	South Island, New Zealand	*Nothofagus truncata*	41°31′ S/172°45′ E	Component Carbon Analyses	2.84	Waring et al. (1998)
	EUROFLUX Network	Various Species[6]	41°–64° N/0°–24° E	Component Carbon Analyses	3.78	Janssens et al. (2001)
	Massachusetts, USA	Deciduous Forest[7]	42°32′ N/72°11′ W	Component Carbon Analyses	3.50	Waring et al. (1998)
	The Oregon Transect	Coniferous, Deciduous[8]	44°–45° N/121°–123° W	Component Carbon Analyses	3.80	Williams et al. (1997)
	Colorado, USA (800/1.5)	Mixed Forest[9](100)	–/–	SIPNET Model	2.25	Hu et al. (2010)
		Mixed Forest[5](100)	–/–	SFSI[10]	0.94	Hu et al. (2010)

[1] P denotes annual rainfall amount; T_a denotes refers to average annual temperature.

[2] The dominant species are *Pinus elliottii*, *Pinus massoniana*, *Cunninghamia lanceolata*, and *Schima superba*.

[3] CEVSA is the abbreviation for Carbon Exchange in the Vegetation-Soil-Atmosphere Model.

[4] The even-aged *P. taeda* L. forest was planted in a clear-cut opening in 1983, with additional tree species representing seed sources of pine and broadleaf species from the surrounding area.

[5] 4C-A is the abbreviation for canopy conductance-constrained carbon assimilation.

[6] Sites of the European EUROFLUX network encompass a large range in tree species, such as *Fagus sylvatica*, *Quercus ilex*, *Quercus robur*, *Picea abies* etc.

[7] The dominant species are *Quercus rubra* and *Acer rubrum*.

[8] Dominant species at six coniferous forest and one deciduous forest sites are 1, *Picea sitchensis*, *Tsuga heterophylla*; 2, *Alnus rubra*; 3, *Pseudotsuga menziesii*; 4, *Tsuga heterophylla*, *Pseudotsuga menziesii*; 5, *Tsuga mertensiana*, *Abies lasiocarpa*, *Picea engelmanii*; 6, *Pinus ponderosa*; 7, *Juniperus occidentalis*.

[9] The dominant species are lodgepole pine, subalpine fir, Engelmann spruce.

[10] SFSI is the abbreviation for gas exchange and sap flux/stable isotope.

Table 5. Statistical results from the sensitivity analysis.

	R^2	p	Equation
G_s and F_{CO_2}	0.8263	< 0.0001	$F_{CO_2} = 0.0531 G_s - 0.002$
C_a and F_{CO_2}	0.0016	0.0001	$F_{CO_2} = 0.004 C_a + 0.239$
Δ and F_{CO_2}	0.1348	< 0.0001	$F_{CO_2} = -0.3794\Delta + 10.2506$

F_{CO_2}, canopy CO_2 uptake rate; G_s, canopy stomatal conductance; C_a, ambient CO_2 concentration; Δ, photosynthetic ^{13}C discrimination.
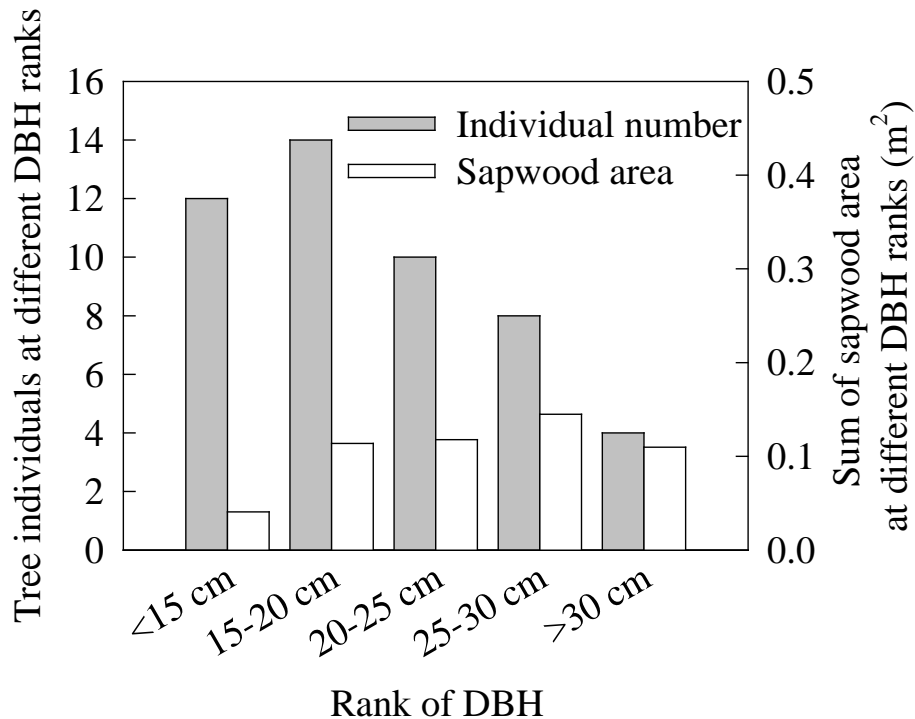
Fig. 1. Frequency distribution of trees and sum of sapwood area of all trees of different diameter at breast height (DBH) ranks at the studied site.

Full Screen / Esc

Printer-friendly Version

Interactive Discussion
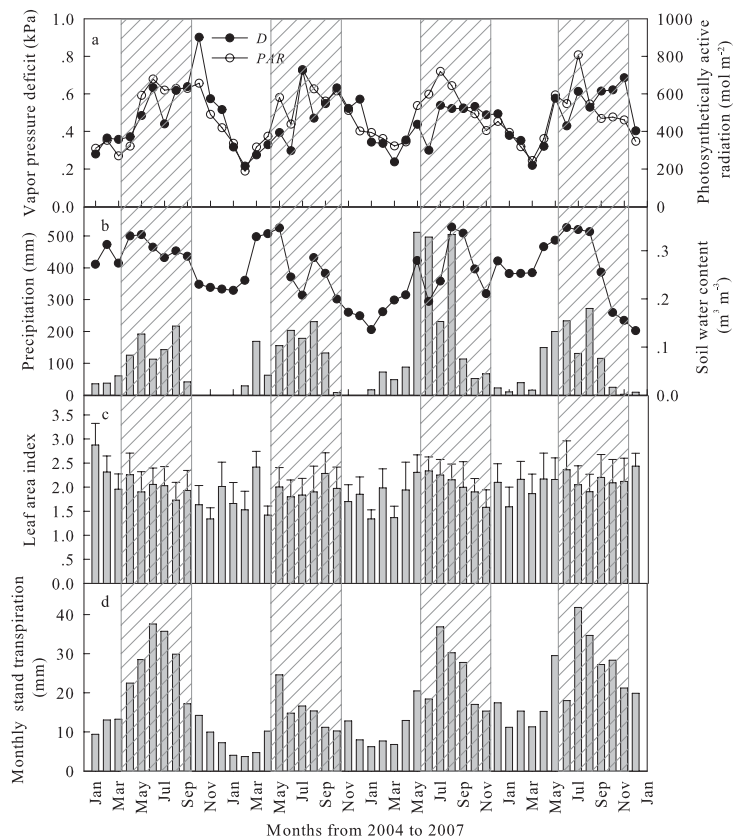
Fig. 2. (a) Monthly mean vapor pressure deficit (*D*), photosynthetically active radiation (PAR) at experimental site; **(b)** precipitation (*P*), monthly mean soil water content (SWC) at experimental site; **(c)** monthly mean leaf area index (LAI) and **(d)** stand transpiration (*E*$_L$) of *A. mangium*. Error bars indicate standard deviation (*n* = 20). Boxes filled with coarse pattern in grey color indicate wet season.

Full Screen / Esc

Printer-friendly Version

Interactive Discussion
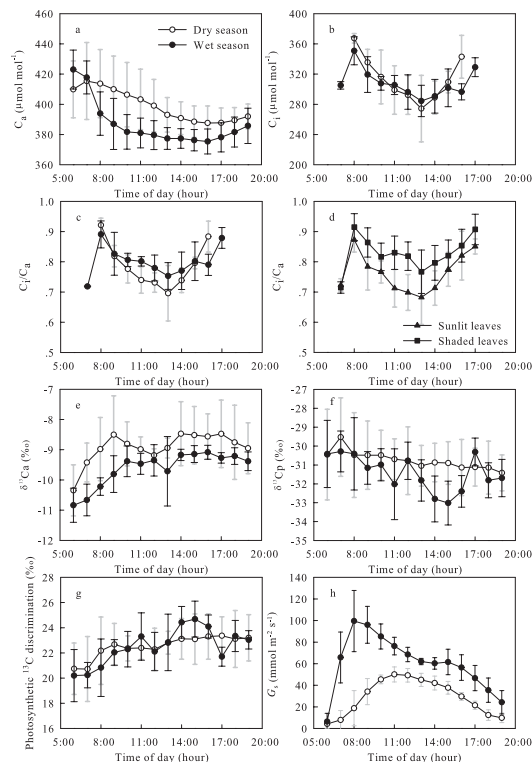
Fig. 3. Diurnal variations of **(a)** ambient CO$_2$ concentration (C_a), **(b)** intercellular CO$_2$ concentration (C_i), **(c)** the ratio of the intercellular and ambient CO$_2$ concentrations (C_i/C_a), **(d)** C_i/C_a in the sunlit and shaded leaves in all seasons, **(e)** carbon isotope compositions in canopy atmosphere ($\delta^{13}C_a$), **(f)** carbon isotope compositions in leaf sap ($\delta^{13}C_p$), and **(g)** photosynthetic ^{13}C discrimination (Δ), and **(h)** canopy stomatal conductance (G_s) in both wet season (9 and 10 May, 26 July, 1 August) and dry season (6 and 7 November, 6 and 17 December). Error bars indicate standard deviation ($n = 8$).
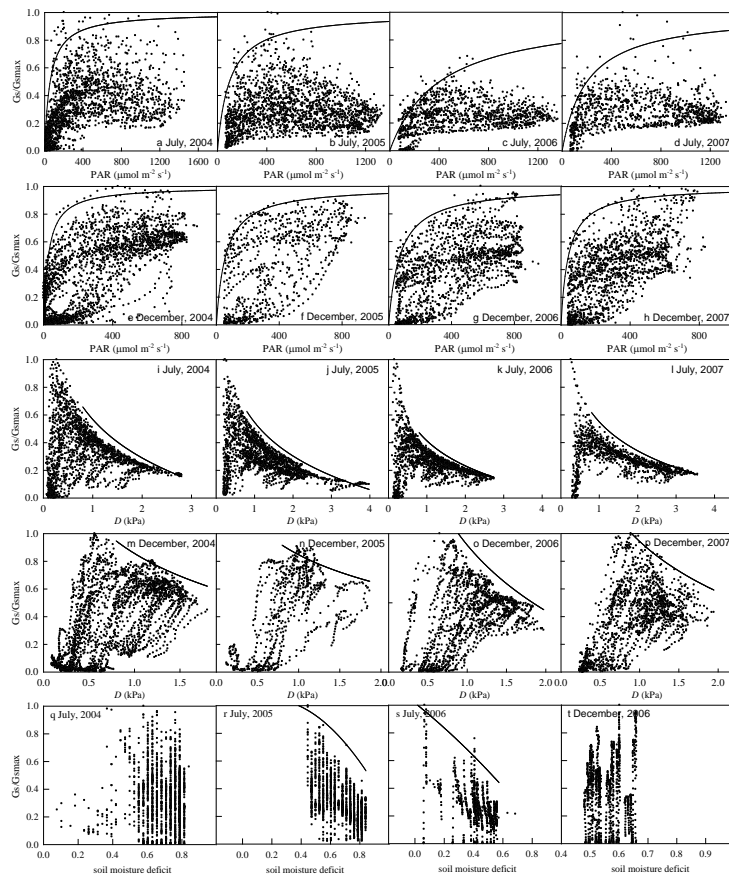
Fig. 4. Scatter plots and response functions of the ratio of canopy stomatal conductance to the maximum (G_s/G_{smax}) to changes in photosynthetically active radiation PAR **(a–h)**, vapor pressure deficit D **(i–p)**, and soil moisture deficit SMD **(q–t)** in both wet season and dry season from 2004–2007.
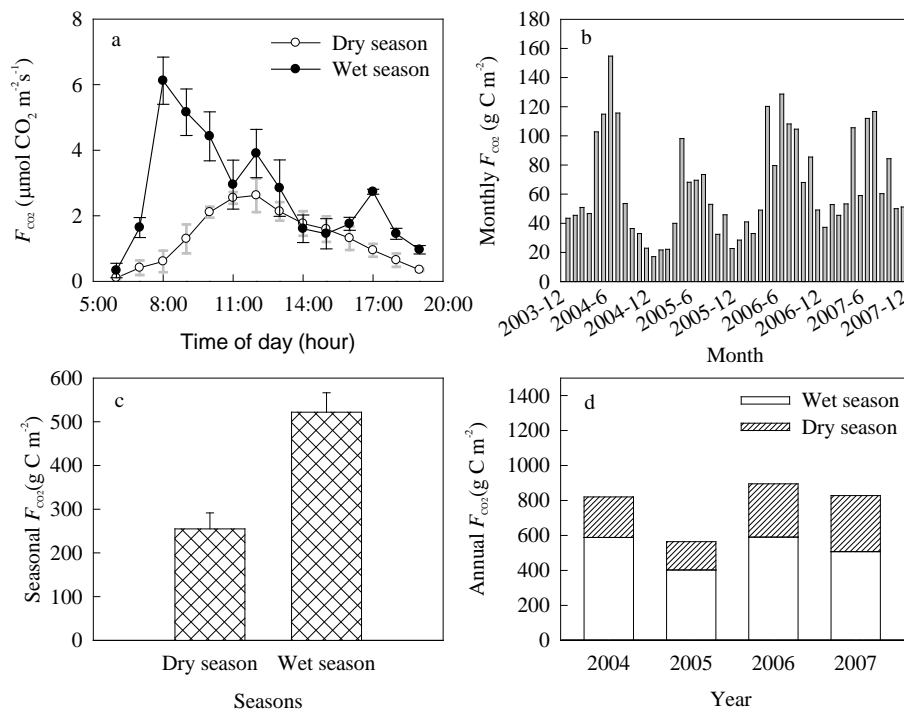
Fig. 5. Diurnal, monthly, seasonal, and annual trends of canopy CO_2 uptake rate (F_{CO_2}) of *A. mangium* plantation from 2004 to 2007. Error bars indicate standard error.
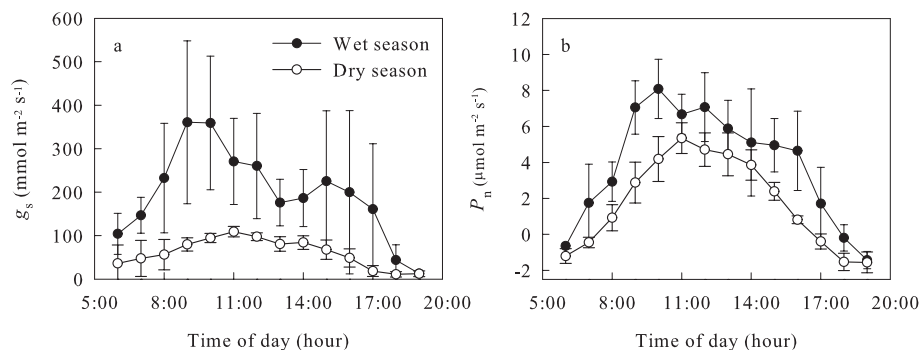
Fig. 6. Diurnal patterns of leaf stomatal conductance (g_s) and net photosynthesis (P_n) of *A. mangium* in both wet season (9 and 10 May, 26 July, 1 August) and dry season (6 and 7 November, 6 and 17 December). Error bars indicate standard deviation ($n = 4$).
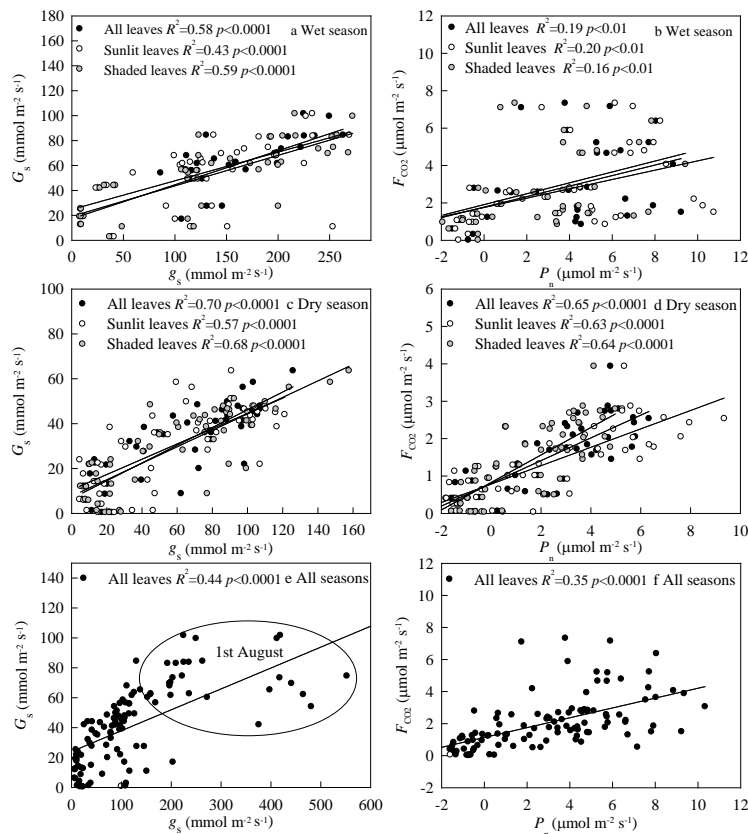
Fig. 7. Scatter plots of leaf stomatal conductance (g_s) vs canopy stomatal conductance (G_s), and leaf net photosynthesis (P_n) vs. canopy CO_2 uptake (F_{CO_2}) in **(a, b)** wet season (9 and 10 May, 26 July), **(c, d)** dry season (6 and 7 November, 6 and 17 December), and **(e, f)** all seasons (9 and 10 May, 26 July, 1 August, 6 and 7 November, 6 and 17 December). The data in eclipse in **(e)** occurred on 1 August.
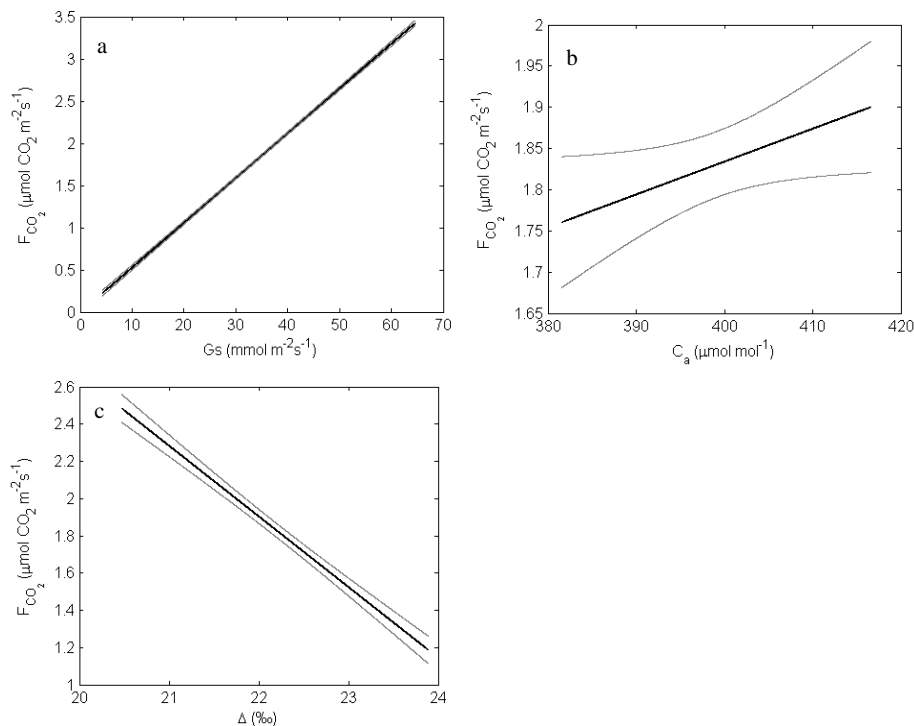
Title Page

Abstract | Introduction

Conclusions | References

Tables | Figures

|◄ | ►|

◄ | ►

Back | Close

Full Screen / Esc

Printer-friendly Version

Interactive Discussion

Fig. 8. Canopy CO_2 uptake rate (F_{CO_2}) sensitivity analysis. The bold black lines are the regression relationships and the gray thin lines are the 95 % confidence intervals for the data. **(a)** Relationship between canopy stomatal conductance (G_s) and F_{CO_2} ($R^2 = 0.8263$, $p < 0.0001$). **(b)** Relationship between ambient CO_2 concentrations (C_a) and F_{CO_2} ($R^2 = 0.0016$, $p = 0.0001$). **(c)** Relationship between photosynthetic ^{13}C discrimination (Δ) and F_{CO_2} ($R^2 = 0.1348$, $p < 0.0001$).

Title Page

Abstract | Introduction

Conclusions | References

Tables | Figures

|◄ | ►|

◄ | ►

Back | Close

Full Screen / Esc

Printer-friendly Version

Interactive Discussion